

BEPPoSAX OBSERVATIONS OF UNPRECEDENTED SYNCHROTRON ACTIVITY IN THE
BL LACERTAE OBJECT MARKARIAN 501

ELENA PIAN,^{1,2} GIUSEPPE VACANTI,³ GIANPIERO TAGLIAFERRI,⁴ GABRIELE GHISELLINI,⁴ LAURA MARASCHI,⁵ ALDO TREVES,⁶ C. MEGAN URRY,¹ FABRIZIO FIORE,⁷ PAOLO GIOMMI,⁷ ELIANA PALAZZI,² LUCIO CHIAPPETTI,⁸ AND RITA M. SAMBRUNA⁹

Received 1997 August 1; accepted 1997 October 23; 1997 November 14

ABSTRACT

The BL Lacertae object Markarian 501, one of only three extragalactic sources (with Mrk 421 and 1ES 2344+514) so far detected at TeV energies, was observed with the *BeppoSAX* satellite in 1997 April 7, 11, and 16 during a phase of high activity at TeV energies, as monitored with the Whipple, HEGRA, and CAT Cherenkov telescopes. Over the whole 0.1–200 keV range, the spectrum was exceptionally hard ($\alpha \leq 1$, with $F_\nu \propto \nu^{-\alpha}$), indicating that the X-ray power output peaked at (or above) ~ 100 keV. This represents a shift of at least 2 orders of magnitude with respect to previous observations of Mrk 501, a behavior never seen before in this or any other blazar. The overall X-ray spectrum hardens with increasing intensity, and at each epoch it is softer at larger energies. The correlated variability from soft X-rays to the TeV band points to models in which the same population of relativistic electrons produces the X-ray continuum via synchrotron radiation and the TeV emission by inverse Compton scattering of the synchrotron photons or other seed photons. For the first time in any blazar, the synchrotron power is observed to peak at hard X-ray energies. The large shift of the synchrotron peak frequency with respect to previous observations of Mrk 501 implies that intrinsic changes in the relativistic electron spectrum caused the increase in emitted power. Due to the very high electron energies, the inverse Compton process is limited by the Klein-Nishina regime. This implies a quasi-linear (as opposed to quadratic) relation of the variability amplitude in the TeV and hard X-ray ranges (for the synchrotron self-Compton model) and an increase of the inverse Compton peak frequency smaller than that of the synchrotron peak frequency.

Subject headings: BL Lacertae objects: individual (Markarian 501) — galaxies: active — galaxies: nuclei — radiation mechanisms: nonthermal — X-rays: galaxies

1. INTRODUCTION

Markarian 501 is one of the closest ($z = 0.034$) BL Lacertae objects, and one of the brightest at all wavelengths. It was the second source, after Mrk 421, to be detected at TeV energies by the Whipple and HEGRA observatories (Quinn et al. 1996; Bradbury et al. 1997). Historically, its spectral energy distribution (νF_ν) resembles that of BL Lac objects selected at X-ray energies, having a peak in the EUV-soft X-ray energy band. Such objects were defined as high-frequency-peaked BL Lac objects, or HBLs, by Padovani & Giommi (1995). In fact, the 2–10 keV spectra observed so far were relatively steep, with energy spectral indices α larger than unity ($F_\nu \propto \nu^{-\alpha}$), meaning that the power output peaks below this band. From the *EXOSAT* database, the hardest X-ray spectrum of Mrk 501, measured in one of its brightest states, had a spectral index of 1.2 ± 0.1 (Sambruna et al. 1994). In two occasions, the *Einstein* satellite

took measurements of spectral indices that were consistent with values smaller than 1 within the large errors (Urry, Mushotzky, & Holt 1986). Mrk 501 was observed with *BeppoSAX* over a period of ~ 10 hr each day in 1997 April 7, 11, and 16, during a multiwavelength campaign involving ground-based TeV Cherenkov telescopes (Whipple, HEGRA and CAT), plus other satellites (*Compton Gamma Ray Observatory* [EGRET and OSSE], *Rossi X-Ray Timing Explorer*, and *Infrared Space Observatory*) and optical telescopes. The first results on the TeV observations are presented in Catanese et al. (1997), Aharonian et al. (1997a), and Barrau et al. (1997). Infrared, optical, and radio data from the multiwavelength campaign, as well as a complete analysis of the *BeppoSAX* data, including a detailed study of the intraday X-ray variability, will be presented in forthcoming papers. Here we concentrate on the average spectra obtained during the three *BeppoSAX* pointings. In the X-ray band, unprecedented spectral behavior is observed, offering new constraints on blazar emission mechanisms.

2. OBSERVATIONS, ANALYSIS, AND RESULTS

A complete description of the *BeppoSAX* mission is given by Boella et al. (1997). Mrk 501 was observed with the LECS (0.1–10 keV), the MECS (1.5–11 keV), and the PDS (13–300 keV). Event files of the three *BeppoSAX* pointings for the LECS and MECS experiments were linearized and cleaned with SAXDAS at the *BeppoSAX* Science Data Center (SDC; Giommi & Fiore 1997). Light curves and spectra were accumulated for each pointing with the SAXSELECT tool, using 8'5 and 4' extraction radii for the LECS and the MECS, respectively, that provide more than 90% of the fluxes. The background intensity was evaluated from files accumulated from blank fields available at the SDC. For each of the four PDS units, source plus background and background spectra were

¹ Space Telescope Science Institute, 3700 San Martin Drive, Baltimore, MD 21218; pian@stsci.edu, cmu@stsci.edu.

² Istituto di Tecnologie e Studio delle Radiazioni Extraterrestri, CNR, via Gobetti 101, I-40129 Bologna, Italy; eliana@tesre.bo.cnr.it.

³ European Space Agency-ESTEC, Space Science Department, Astrophysics Division, Postbus 299, 2200 AG Noordwijk, The Netherlands; gvacanti@astro.estec.esa.nl.

⁴ Osservatorio Astronomico di Brera, Via E. Bianchi 46, I-22055 Merate (Lecco), Italy; gtagliaf@astmim.mi.astro.it, gabriele@merate.mi.astro.it.

⁵ Osservatorio Astronomico di Brera, via Brera 28, I-20121 Milano, Italy; maraschi@brera.mi.astro.it.

⁶ Department of Physics, University of Milan at Como, Via Lucini 3, I-22100 Como, Italy; treves@astmiu.mi.astro.it.

⁷ SAX SDC, Via Corcolle 19, I-00131, Rome, Italy; fiore@sax.sdc.asi.it, giommi@sax.sdc.asi.it.

⁸ Istituto di Fisica Cosmica CNR, via Bassini, 15, I-20133 Milano, Italy; lucio@ifctr.mi.cnr.it.

⁹ NASA/Goddard Space Flight Center, Greenbelt, MD 20771; rms@latte.astro.psu.edu.

TABLE 1
SPECTRAL FITS^a TO LECS + MECS AND PDS DATA

PARAMETER	OBSERVATION START–END ^b		
	7.2295–7.6679	11.2458–11.6846	16.1506–16.6082
α^c	0.80 ± 0.01	0.74 ± 0.01	0.52 ± 0.01
$\chi_r^2 (N_{\text{dof}})$	3.4 (180)	1.78 (180)	2.77 (180)
$\alpha_1 (E < E_{\text{break}})^d$	0.63 ± 0.04	$0.64^{+0.02}_{-0.04}$	$0.40^{+0.02}_{-0.04}$
$\alpha_2 (E > E_{\text{break}})^d$	0.91 ± 0.02	0.80 ± 0.02	$0.59^{+0.02}_{-0.01}$
$E_{\text{break}} (\text{keV})$	$1.76^{+0.24}_{-0.22}$	1.85 ± 0.33	$2.14^{+0.30}_{-2.14}$
$\chi_r^2 (N_{\text{dof}})$	1.29 (178)	1.00 (178)	1.33 (178)
α_{PDS}	0.99 ± 0.13	$0.83^{+0.09}_{-0.08}$	$0.84^{+0.03}_{-0.04}$
$\chi_r^2 (N_{\text{dof}})$	0.92 (12)	1.60 (12)	1.09 (12)
$S_{0.1-2 \text{ keV}}^e$	1.75 ± 0.01	1.75 ± 0.01	2.55 ± 0.01
$S_{2-10 \text{ keV}}^e$	2.20 ± 0.01	2.45 ± 0.01	5.35 ± 0.01
$S_{13-200 \text{ keV}}^e$	3.75 ± 0.15	5.15 ± 0.15	15.8 ± 0.2

^a $F_\nu \propto \nu^{-\alpha}$. Errors are at 90% confidence level for one ($\Delta\chi^2 = 2.71$) or three ($\Delta\chi^2 = 6.1$) parameters of interest.

^b 1997 April 7, 11, and 16.

^c Energy index from the single power-law fit to combined LECS and MECS data.

^d Energy index from the broken power-law fit to combined LECS and MECS data.

^e Unabsorbed intensities, in units of 10^{-10} ergs $\text{s}^{-1} \text{cm}^{-2}$, derived from the broken power-law model fit.

accumulated using the XAS software package, after selecting the source visibility windows. The target was significantly detected up to the highest energy channels. Each net spectrum was binned in energy intervals to reach a signal-to-noise ratio larger than 20, up to 150 keV. The grouped spectra from the four units were then co-added.

Spectral analysis was performed with the XSPEC 9.01 package, using the response matrices released by the SDC for each instrument. LECS data have been considered only in the range 0.1–4 keV, because of the still unsolved calibration problems at higher energies, and MECS data in the range 1.8–10.5 keV. For each observation, the LECS and MECS spectra have been jointly fitted after allowing for a constant, systematic rescaling factor of the LECS data to account for uncertainties in the intercalibration of the instruments (A. N. Parmar 1997, private communication), which had a best-fit value 0.64. This factor was derived by comparing the responses of LECS and MECS

in their common energy range. We considered both simple and broken power-law models, the latter is appropriate for HBLs, which often show downward-curved spectra. With the former model, the fitted N_{H} is 30%–40% higher than the Galactic value ($1.73 \times 10^{20} \text{ cm}^{-2}$; Elvis, Lockman, & Wilkes 1989), while the broken power-law model yields a value equal to the Galactic one for the first two observations and a somewhat lower value ($\sim 20\%$) for the third one. We then fixed N_{H} at the Galactic value and determined the best-fit parameters for both the single and broken power-law models (see Table 1): the latter is clearly in all cases a better representation of the data (the χ^2 improvement is highly significant as estimated from the F -test). The spectral steepening is of $\Delta\alpha \approx 0.2$ – 0.3 at all epochs. Single power laws represent well the PDS spectra in the 13–200 keV range (see fit parameters in Table 1) at each epoch. For April 7 and 11, the PDS slopes are consistent with the energy indices derived from the broken power-law LECS + MECS best fits (α_2 in Table 1), while for April 16 the spectrum in the 13–200 keV band is significantly steeper than in the MECS band. After rescaling the PDS data by a factor 0.75 in order to take into account a calibration mismatch with respect to the MECS response, we fitted the April 16 spectrum over the whole range (LECS + MECS + PDS) with a broken power-law model. The PDS data show a systematic deviation from the model (Fig. 1a), indicating a further steepening at higher energies. Figure 1b shows a joint fit only to the MECS + PDS data with a broken power law with break energy of ~ 20 keV: the spectral indices on the lower and higher energy side of the break (see figure caption) are similar to α_2 and α_{PDS} (Table 1), respectively.

In order to characterize the spectral variability in the full range, independent of calibration uncertainties or model assumptions, we computed the ratio of the count rates observed on April 16 to those observed on April 7 versus energy, as shown in Figure 2. It is clear that the variability is systematically larger at higher energies, implying an overall hardening of the spectrum with increasing intensity, by about $\Delta\alpha \approx 0.2$ in each band (see Table 1). In April 7 and 11, the spectral index in the PDS band is consistent with $\alpha \approx 1$, while on April 16 it is less than unity, indicating that the peak of the power output falls in the PDS band at the first two epochs but is at

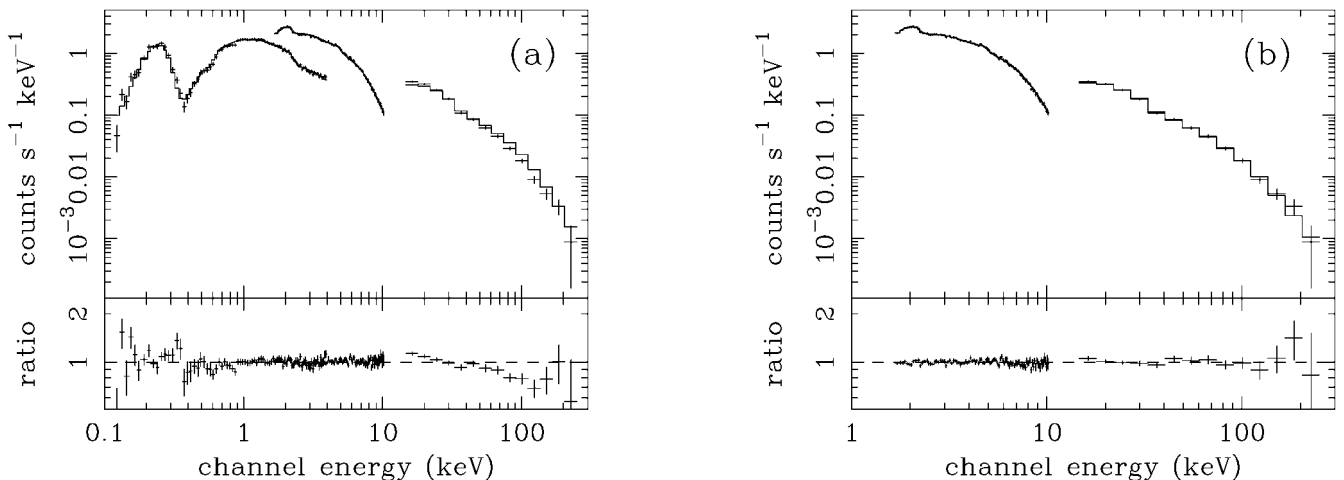


FIG. 1.—(a) Broken power-law fit to the LECS + MECS + PDS data of 1997 April 16. The top panel shows the spectra from each instrument (see Table 1 for the parameters); the bottom panel shows the ratio between the spectral flux distribution and the model. (b) Same as in (a), but for the MECS + PDS data of April 16: best-fit spectral indices at energies lower and higher than the break energy of $19.5^{+4.5}_{-3.5}$ keV are $0.58^{+0.03}_{-0.02}$ and $0.83^{+0.08}_{-0.06}$, respectively ($\chi_r^2 = 1.24$ for 113 degrees of freedom [dof]).

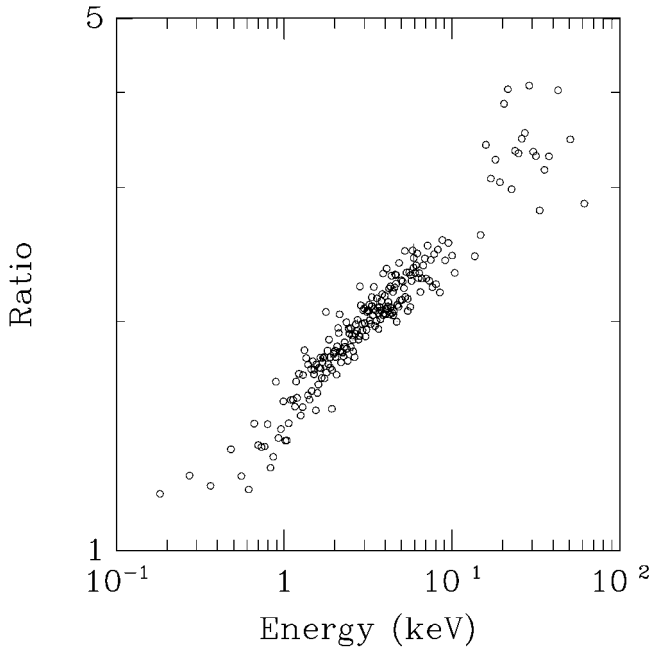


FIG. 2.—Ratio of the LECS + MECS + PDS spectra of April 7 and 16. The hardening of the April 16 spectrum is clearly evident.

the extreme end of the PDS band or beyond in the highest intensity state.

3. SPECTRAL ENERGY DISTRIBUTION

In Figure 3, the unfolded and unabsorbed X-ray spectra from the *BeppoSAX* observations of April 7 and 16 are compared with previously observed X-ray spectra in three brightness states and with data from the radio to the TeV range (see figure caption for references). The present X-ray observations imply a dramatic hardening of the spectral energy distribution in the medium X-ray band and an increase of the (apparent) bolometric luminosity of a factor ≥ 20 with respect to previous epochs. The really striking feature is that the peak of the power output (i.e., where $\alpha = 1$) has shifted in energy by a factor ≥ 100 . Moreover, for the first time in any blazar, the peak is observed to occur in the hard X-ray range, definitely above ~ 50 – 100 keV (cf. Ulrich, Maraschi, & Urry 1997). Since, in the optical, the source was nearly normal (Buckley & McEney 1997), the change of the spectral energy distribution seems to be confined to energies greater than ~ 0.1 keV, as also indicated by the apparent pivot of the three *BeppoSAX* spectra. The overall continuity of the X-ray spectra reported here with previous UV and soft X-ray measurements suggests that the X-ray emission constitutes the high-energy end of the synchrotron component, and thus that its peak frequency increased by more than 2 orders of magnitude and its power by more than 1 order of magnitude with respect to previous observations of Mrk 501. The TeV emission also brightened by more than a factor of 5 in the first 2 weeks of April, with the most intense TeV flare peaking on April 16 (Catanese et al. 1997), the date of the last *BeppoSAX* observation. However, unlike the X-ray spectrum, the TeV spectrum was steeper than $\alpha = 1$ and did not show noticeable temporal variation; from the HEGRA measurements during the period of March–April and during the more active period of April 7–13, the spectral index above 1 TeV remained unchanged, within the large errors ($\Delta\alpha \sim 0.3$), with an average

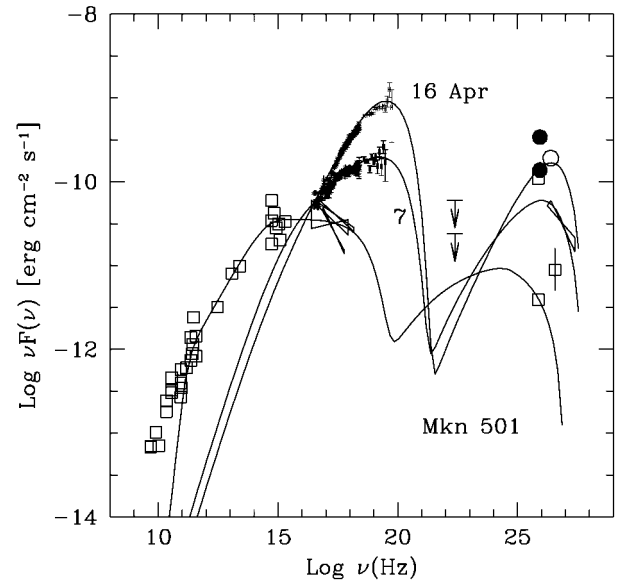


FIG. 3.—Spectral energy distribution of Mrk 501. The *BeppoSAX* data from 1997 April 7 and 16 are indicated as labeled. The nearly simultaneous Whipple TeV data (from Catanese et al. 1997) are indicated as filled circles, while the open circle (1997 April 13) and the TeV spectral fit (1997 March 15–20), along with its 1σ confidence range, are from the HEGRA experiment (Aharonian et al. 1997a). Nonsimultaneous measurements collected from the literature are shown as open squares (radio: Gear et al. 1994; millimeter: Steppe et al. 1988, Wiren et al. 1992, Lawrence et al. 1991, and Bloom & Marscher 1991; far-infrared: Impey & Neugebauer 1988; optical: Véron-Cetty & Véron 1993 and Burbidge & Hewitt 1987; UV: Pian & Treves 1993; TeV: Quinn et al. 1996, Breslin et al. 1997, and Bradbury et al. 1997). X-ray spectral fits range in the low state are from Sambruna et al. 1994, Worrall & Wilkes 1990, and Comastri et al. 1997. Upper limits at 100 MeV are from Weekes et al. 1996 and Catanese et al. 1997. The solid lines indicate fits with a one-zone, homogeneous synchrotron self-Compton model. For all models, the size of the emitting region is $R = 5 \times 10^{15}$ cm, the beaming factor is $\delta = 15$, and the magnetic field is $B \sim 0.8$ G. For the “quiescent state,” the intrinsic luminosity (corrected for beaming) is $L' = 4.6 \times 10^{40}$ ergs s^{-1} , and electrons are continuously injected with a power-law distribution ($\propto \gamma^{-2}$) between $\gamma_{\min} = 3 \times 10^3$ and $\gamma_{\max} = 6 \times 10^5$. For the fit to the April 7 spectrum, $L' = 1.8 \times 10^{41}$ ergs s^{-1} , and the injected electron distribution ($\propto \gamma^{-1.5}$) extends from $\gamma_{\min}^4 = 1 \times 10^4$ to $\gamma_{\max} = 3 \times 10^6$. For the fit to the April 16 spectrum, $L' = 5.5 \times 10^{41}$ ergs s^{-1} , and the injected electron distribution ($\propto \gamma^{-1}$) extends from $\gamma_{\min} = 4 \times 10^5$ to $\gamma_{\max} = 3 \times 10^6$. For the April 7 and 16 models, the seed photons for the Compton scattering are the sum of those produced by the assumed electron distribution plus those corresponding to the quiescent spectrum.

value $\alpha \approx 1.5$ (Aharonian et al. 1997a, 1997b). At the same time, Mrk 501 was not detected by EGRET (Catanese et al. 1997), indicating that the γ -ray flare is modest at a few GeV. This constrains the peak power output of the very high energy component to occur between the GeV and TeV ranges. Note that also during the quiescent state, the latter peak was poorly constrained so that it is difficult to make a strong statement about a possible shift. In the quiescent state, the TeV flux was a factor ~ 100 less than during the flare of April 16.

4. MODEL IMPLICATIONS

The spectral energy distribution of HBLs can be well explained by the synchrotron self-Compton model, in which the dominant source of seed photons is the synchrotron emission (Jones, O’Dell, & Stein 1974; Ghisellini, Maraschi, & Dondi 1996; Mastichiadis & Kirk 1997). If the energy distribution of the emitting electrons, $N(\gamma)$, changes at the highest energies, this model explains naturally the correlated flaring at X-ray and

TeV energies, with the highest energy electrons producing X-rays via synchrotron and the TeV radiation via inverse Compton scattering. Because of the very high electron energies involved, the scattering cross section for energetic photons is reduced by the Klein-Nishina effect, and only photons below the Klein-Nishina threshold ($h\nu \leq mc^2/\gamma$) are effectively upscattered. This means that (i) the inverse Compton flux does not vary more than the synchrotron flux from the same electrons, since the available seed photons are limited (Ghisellini & Maraschi 1996), and that (ii) the peak of the inverse Compton power shifts less in frequency than the synchrotron peak, which depends on the square of the electron energy.

The shift of ~ 2 orders of magnitude in the frequency ν_s of the synchrotron peak of Mrk 501 cannot be ascribed to a variation of either Doppler factor δ or magnetic field B alone; enormous variations would be demanded, since $\nu_s \propto B\delta$, and these changes would affect other parts of the spectrum quite strongly in a way that is not observed. Therefore, a real change in power and an increase in maximum electron energy are implied. Assuming that the power variation is only due to a change in the electron energy, γ_{\max} must have increased by roughly a factor of ~ 10 – 30 . The corresponding shift of the inverse Compton peak is expected to be of the same order of magnitude, being in the Klein-Nishina regime. Since the cooling time of these very high energy electrons is rather short, and the synchrotron peak did not move back to the quiescent position during at least 10 days, a mechanism of continuous particle injection is required. This could be impulsive acceleration of electrons at a shock triggered by fluctuations in the velocity or energy of newly injected plasma. In the γ -ray-emitting region, therefore, the fresh electrons would scatter not only the synchrotron photons, but also a preexisting (and more stationary) photon population, produced by an older electron distribution. The hard X-ray and TeV emission should then vary with similar amplitude, while the flux in the infrared-optical band could remain almost stationary.

Three one-zone synchrotron self-Compton models along these lines are shown in Figure 3 for the quiescent state and the April 7 and 16 states. The $N(\gamma)$ distribution has been found self-consistently, solving the continuity equation that included continuous injection of relativistic particles, radiative losses, and electron-positron pair production and taking into account

the Klein-Nishina cross section (Ghisellini 1989). The parameters of the fits are given in the figure caption. A variation of the maximum energy of the emitting electrons, together with an increased luminosity and a flattening of the injected particle distribution, can describe the observed flaring spectra quite well. We assumed that the seed photons for the inverse Compton scattering are the sum of those produced by the injected electrons plus a stationary component, comparable to the observed infrared-optical flux, which is assumed to be cospatial with the high-energy emission. This component can be associated with the “quiescent” spectrum. We recall that these one-zone models cannot account for the radio emission that is thought to be produced in much larger regions of the source. We note that the soft X-ray flux (up to a few keV) did not vary dramatically, and that soft X-ray observations alone would have failed to recognize an unusual behavior, except for measuring a spectral inversion, namely, a change in slope from values larger than 1 to values smaller than 1. In the *EXOSAT* database (Sambruna et al. 1994), at least two sources (out of 16) show spectral indices smaller than 1 in the medium-energy X-ray range, but in the brightest and most frequently observed sources (i.e., with more than 10 spectra, which is the case also for Mrk 501), such behavior was never observed. Thus, flares as discovered in Mrk 501 may occur in other (similar) blazars, although not very frequently, and/or some blazars may be more often in ultrahard states. The signature would be a flat slope in the X-rays, with a flux level consistent with the extrapolation of the infrared-optical synchrotron spectrum. These sources should be the most variable in hard X-rays and the strongest ones in the TeV band; therefore, their investigation with the existing and rapidly developing X-ray and γ -ray instrumentation is one of the most promising projects of high-energy astronomy.

We thank F. Aharonian for a critical reading of the manuscript and for providing helpful comments and suggestions, and M. Catanese for sending us, on behalf of the Whipple team, his manuscript in advance of submission. J. Buckley, G. Fossati, K. O’Flaherty, M. Schubnell, and T. Weekes are acknowledged for their support of this project. C. M. U. and E. Pian acknowledge support from NASA grants NAG5-2510 and NAG5-2538.

REFERENCES

- Aharonian, F., et al. 1997a, *A&A*, in press
 ———. 1997b, in *Proc. Fourth Compton Symp.*, ed. C. A. Meegan & P. Cushman (New York: AIP), in press
 Barrau, A., et al. 1997, 25th Int. Cosmic Ray Conf. (Durban), in press (astro-ph/9705249)
 Bloom, S. D., & Marscher, A. P. 1991, *ApJ*, 366, 16
 Boella, G., Butler, R. C., Perola, G. C., Piro, L., Scarsi, L., & Bleeker, J. A. M. 1997, *A&AS*, 122, 299
 Bradbury, S. M., et al. 1997, *A&A*, 320, L5
 Breslin, A. C., et al. 1997, *IAU Circ.* 6592
 Buckley, J., & McEnery, J. 1997, in preparation
 Burbidge, G., & Hewitt, A. 1987, *AJ*, 93, 1
 Catanese, M., et al. 1997, *ApJ*, 487, L143
 Comastri, A., Fossati, G., Ghisellini, G., & Molendi, S. 1997, *ApJ*, 480, 534
 Elvis, M., Lockman, F. J., & Wilkes, B. J. 1989, *AJ*, 97, 777
 Gear, W. K., et al. 1994, *MNRAS*, 267, 167
 Ghisellini, G. 1989, *MNRAS*, 236, 341
 Ghisellini, G., & Maraschi, L. 1996, in *ASP Conf. Ser. 110, Blazar Continuum Variability*, ed. H. R. Miller, J. R. Webb, & J. C. Noble (San Francisco: ASP), 436
 Ghisellini, G., Maraschi, L., & Dondi, L. 1996, *A&AS*, 120, 503
 Giommi, P., & Fiore, F. 1997, *Proc. Fifth Int. Workshop on Data Analysis in Astronomy*, ed. V. Di Gesù, M. J. B. duff, A. Heck, M. C. Maccarone, L. Scarsi, H. U. Zimmerman (Singapore: World Scientific), in press
 Impey, C. D., & Neugebauer, G. 1988, *AJ*, 95, 307
 Jones, T. W., O’Dell, S. L., & Stein, W. A. 1974, *ApJ*, 188, 353
 Lawrence, A., Rowan-Robinson, M., Efstathiou, A., Ward, M. J., Elvis, M., Smith, M. G., Duncan, W. D., & Robson, E. I. 1991, *MNRAS*, 248, 91
 Mastichiadis, A., & Kirk, J. G. 1997, *A&A*, 320, 19
 Padovani, P., & Giommi, P. 1995, *ApJ*, 444, 567
 Pian, E., & Treves, A. 1993, *ApJ*, 416, 130
 Quinn, J., et al. 1996, *ApJ*, 456, L83
 Sambruna, R. M., Barr, P., Giommi, P., Maraschi, L., Tagliaferri, G., & Treves, A. 1994, *ApJS*, 95, 371
 Steppe, H., Salter, C. J., Chini, R., Kreysa, E., Brunswig, W., & Lobato Perez, J. 1988, *A&AS*, 75, 317
 Ulrich, M.-H., Maraschi, L., & Urry, C. M. 1997, *ARA&A*, in press
 Urry, C. M., Mushotzky, R. F., & Holt, S. S. 1986, *ApJ*, 305, 369
 Véron-Cetty, M.-P., & Véron, P. 1993, *ESO Scientific Rep. No. 13*, 1
 Weekes, T. C., et al. 1996, *A&AS*, 120, 603
 Wiren, S., Valtaoja, E., Teräsranta, H., & Kotilainen, J. 1992, *AJ*, 104, 1009
 Worrall, D. M., & Wilkes, B. J. 1990, *ApJ*, 360, 396